

# An optical cloak made of dielectrics

Jason Valentine<sup>1\*</sup>, Jensen Li<sup>1\*</sup>, Thomas Zentgraf<sup>1\*</sup>, Guy Bartal<sup>1</sup> and Xiang Zhang<sup>1,2†</sup>

**Invisibility devices have captured the human imagination for many years. Recent theories have proposed schemes for cloaking devices using transformation optics and conformal mapping<sup>1–4</sup>. Metamaterials<sup>5,6</sup>, with spatially tailored properties, have provided the necessary medium by enabling precise control over the flow of electromagnetic waves. Using metamaterials, the first microwave cloaking has been achieved<sup>7</sup> but the realization of cloaking at optical frequencies, a key step towards achieving actual invisibility, has remained elusive. Here, we report the first experimental demonstration of optical cloaking. The optical ‘carpet’ cloak is designed using quasi-conformal mapping to conceal an object that is placed under a curved reflecting surface by imitating the reflection of a flat surface. The cloak consists only of isotropic dielectric materials, which enables broadband and low-loss invisibility at a wavelength range of 1,400–1,800 nm.**

The development of transformation optics has provided new tools to transform space and light propagation using the invariance of Maxwell equations<sup>8,9</sup>. Using transformation optics as the design method<sup>2</sup>, the first experimental demonstration of cloaking was recently achieved at microwave frequencies<sup>7</sup> using metallic ring metamaterials possessing spatially varied magnetic resonances with extreme values for the permeability. Such resonances are naturally accompanied by strong dispersion, resulting in a cloak that works only in a narrow frequency range. In addition, the strong magnetic response obtained in microwave metamaterials<sup>5,6</sup>, where metal is close to being perfect, cannot be sustained at optical frequencies owing to the higher loss and the kinetic inductance of the electrons, prohibiting a simple scaling to optical frequencies<sup>10–12</sup>.

Recently, a number of new forms of cloaking have been proposed to mitigate these constraints<sup>13–17</sup>, relaxing the requirement of extreme material properties. Of special interest is the carpet cloak. Whereas previous cloak designs compress the object into either a singular point or line, the carpet cloak compresses an object in only one direction into a conducting sheet<sup>15</sup>. When the object is under a curved reflecting surface with the carpet cloak on top of it, the object appears as if it is the original flat reflecting surface, so it is hidden under a ‘carpet’. Such a topological change of the cloak avoids both material and geometry singularities<sup>18</sup>. Unlike previous cloaking transformations, it is non-singular and generates a smaller range for the material properties. Quasi-conformal mapping is used so that all of the originally square cells are transformed to rectangles of a constant aspect ratio. Whereas all other mappings result in a highly anisotropic cloak profile, the quasi-conformal mapping can make the transformed cells almost square, so that the anisotropy of the medium is minimized to a point where it can be neglected. This results in a modest range of isotropic indices for the cloak. The approach enables the use of non-resonant elements (such as conventional dielectric materials) and offers the possibility to achieve low-loss and broadband cloaking at optical wavelengths, rendering an object truly undetectable with visible or

infrared light. Carpet cloaking was recently realized experimentally at microwave frequencies, using non-resonant metallic elements<sup>19</sup>. However, even with the advances in optical metamaterials<sup>20–22</sup>, scaling sub-wavelength metallic elements and placing them in an arbitrarily designed spatial manner still remain challenging at optical frequencies.

Here, we experimentally demonstrate optical cloaking using a dielectric carpet cloak design that is not only isotropic, but also low-loss and broadband. The invisibility is demonstrated within a silicon (Si) slab waveguide where the cloak region is obtained by varying the effective index of refraction in a two-dimensional (2D) space. This index profile is designed using quasi-conformal mapping and realized by fabricating a 2D sub-wavelength hole lattice with varying density<sup>23</sup> (see Supplementary Information). The cloak is placed around a reflecting curved surface (bump) and consequently, a light beam incident on the bump shows a reflection profile identical to that of a beam reflected from a flat surface. Therefore, any arbitrarily shaped object placed behind the bump will maintain the reflectance of a smooth, flat surface, rendering the object invisible. This approach represents a major step towards general transformation optics<sup>24–26</sup> at optical frequencies, which has so far remained a challenging endeavour owing to increased metal loss and fabrication limitations, with only basic optical applications (for example, lenses) brought to reality<sup>27–29</sup>. It simplifies the realization of an arbitrary 2D sub-wavelength effective index profile, by using the simple and uniform geometry of a hole array with variable density. This enables easy fabrication and scaling, opening the possibility for a large variety of transformation optics devices at visible and infrared wavelengths. This method eliminates the need for metallic elements and anisotropy with spatial variations at a deep sub-wavelength scale and a size of tens of nanometres.

The carpet cloak metamaterial was fabricated on a silicon-on-insulator (SOI) wafer consisting of a 250-nm-thick silicon layer separated by a 3- $\mu\text{m}$ -thick silicon oxide ( $\text{SiO}_2$ ) slab from a Si wafer substrate (Fig. 1a). The 250 nm Si layer serves as an optical slab waveguide where the light is confined in the vertical dimension and can freely propagate in the other two dimensions. Although this report will focus on the transverse magnetic waveguide mode for the experimental demonstration of cloaking, it is also possible to design the cloak for the transverse electric waveguide mode. The reflecting surface was fabricated by using focused ion beam milling (FIB) to etch through the Si layer and partially through the  $\text{SiO}_2$  slab near the edge of the SOI substrate, making the surface accessible for directional deposition of metal from the side.

The carpet cloak region of the device (Fig. 1a) is composed of a triangular region (marked as C2) with a uniform hole pattern, serving as a background medium with a constant effective index of 1.58, and a rectangular cloak region (marked as C1) with the 2D variable index profile. The hole pattern was created by milling holes of constant diameter (110 nm) through the Si layer with FIB. The holes were milled with varying densities, yielding the desired

<sup>1</sup>NSF Nano-scale Science and Engineering Center (NSEC), 3112 Etcheverry Hall, University of California, Berkeley, California 94720, USA, <sup>2</sup>Material Sciences Division, Lawrence Berkeley National Laboratory, Berkeley, California 94720, USA. \*These authors contributed equally to this work.

†e-mail: xiang@berkeley.edu.

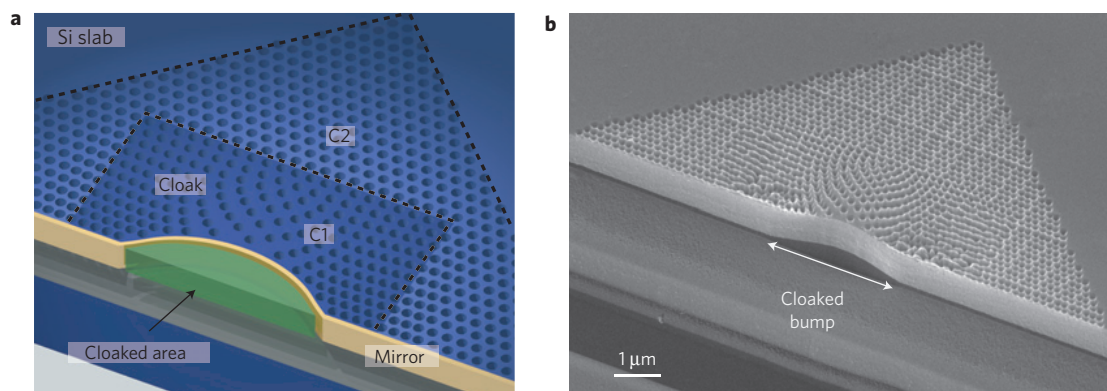


**Figure 1 | The carpet cloak design that transforms a mirror with a bump into a virtually flat mirror.** **a**, Schematic diagram of a fabricated carpet cloak showing the different regions, where C1 is the gradient index cloak and C2 is a uniform index background. The cloak is fabricated in a SOI wafer where the Si slab serves as a 2D waveguide. The cloaked region (marked with green) resides below the reflecting bump (carpet) and can conceal any arbitrary object. The cloak will transform the shape of the bump back into a virtually flat object. **b**, Scanning electron microscope image of a fabricated carpet cloak. The width and depth of the cloaked bump are  $3.8\ \mu\text{m}$  and  $400\ \text{nm}$ , respectively.

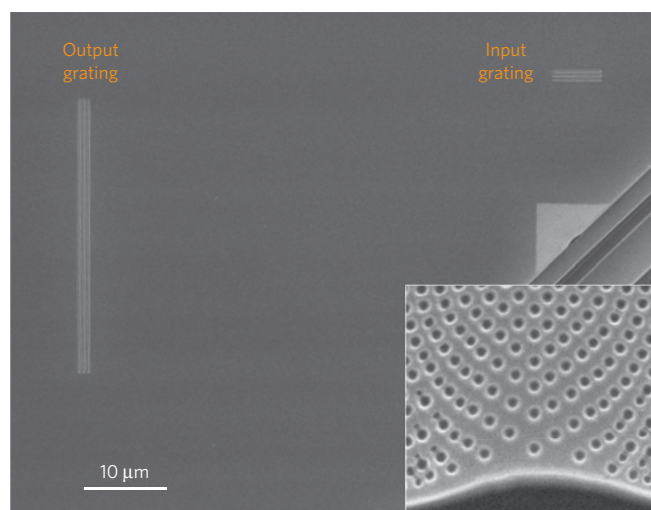


**Figure 2 | Scanning electron microscope image of the carpet cloak layout.** Light is coupled into the Si slab waveguide by the input grating, which has a width of  $7\ \mu\text{m}$  and a distance from the cloak of  $15\ \mu\text{m}$ . After being reflected at the cloaked surface, the beam profile is detected by the output grating, which has a width of  $35\ \mu\text{m}$  and a distance from the cloak of  $55\ \mu\text{m}$ . The inset shows the central region of the cloak. The hole diameter is  $110\ \text{nm}$ .

spatial index profile seen in Fig. 1b. In addition, two gratings were fabricated for coupling the light into and out of the Si waveguide. Directional deposition of  $100\ \text{nm}$  gold (Au) was then carried out using electron beam evaporation to create the reflecting surface. An overall image of the device layout can be seen in Fig. 2.

To unambiguously prove the carpet cloak, we compare the profile of a Gaussian beam reflected from a cloaked bump with that of a similar beam reflected from (1) a flat surface without a cloak and (2) a surface with a bump but without a cloak. The tunable light from a femtosecond synchronously pumped optical parametric oscillator (Spectra-Physics, OPAL) was focused at the input grating to launch the fundamental transverse magnetic wave in the Si slab. A CCD (charged-coupled device) camera was then used to measure the light coupled out of the waveguide at the output grating position.

Figure 3 shows the images for the three configurations as well as the intensity profile at the output grating. As seen in Fig. 3a and b, there is considerable contrast between the reflection from the flat and curved surface. The light reflected from the unclocked

bump shows three distinct spots at the output grating due to the scattering of the bump. The flat surface shows the expected Gaussian beam profile, similar to that of the incident wave. To hide the bump on the surface, the designed cloak pattern was placed around the bump in Fig. 3c. Subsequently, the beam profile at the output grating resembles a single reflected beam as is seen with the flat reflecting surface. This demonstrates that the cloak has successfully transformed the curved surface into a flat surface, giving the observer the impression that the beam was reflected from a flat surface. Owing to the fact that there is no penetration of light into the bump (through the metal layer), any object could be placed behind it and effectively hidden, making the object invisible. Both 3D and 2D simulations were carried out with a commercial finite-element method package (COMSOL) to verify the carpet cloak performance. The 2D simulation results for the three configurations are shown in Fig. 3 (a set of full 3D simulations that show good agreement with the 2D simulations can be found in Supplementary Information). The simulations show the magnitude of the electric field component in the  $z$  direction and show a good agreement with the experimental results. We note that the demonstration of the cloaking effect by using an isotropic profile here is in fact closely connected to the optical conformal mapping in ref. 3 but with the phase information also preserved in our case. To show the angular performance of the cloak, samples were fabricated where the input grating was placed at  $30^\circ$  and  $60^\circ$  with respect to the reflective surface. In both cases, the cloaked bump produced a singular beam at the output as is seen with a flat mirror. The results can be found in Supplementary Information. It is interesting to note that nature can provide us with a simple gradient index profile in one direction, or mirage, to bend the light away from the ground. Whereas the mirage effect can distort the image of a distant object, cloaking of an object on the ground requires an index profile varying in two dimensions to fully conceal the scattering from the object.

As the carpet cloak reported here does not rely on resonant elements, it is expected to be nearly lossless and broadband. Nevertheless, the current nanofabrication technology has a practical limit on the deep sub-wavelength hole size owing to the waveguide thickness, causing scattering. Further losses are encountered owing to possible residual gallium left from the FIB. Consequently, the transmission of the carpet cloaking sample was found experimentally to be 58% at a wavelength of  $1,540\ \text{nm}$ . Nonetheless, we emphasize that this reduced transmission is due to experimental imperfections associated with the technique of drilling the holes (FIB) and is not inherent to this cloaking design method. For example, electron beam lithography could be used in conjunction

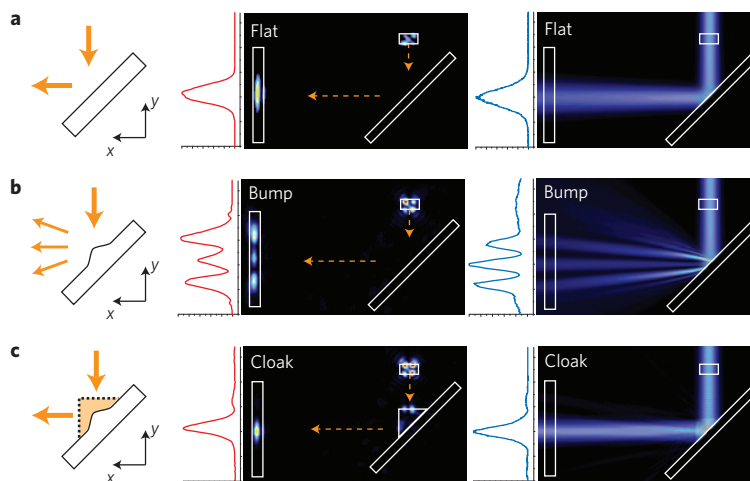


**Figure 3 | Optical carpet cloaking at a wavelength of 1,540 nm. a–c.** The results for a Gaussian beam reflected from a flat surface (**a**), a curved (without a cloak) surface (**b**) and the same curved reflecting surface with a cloak (**c**). The left column shows the schematic diagrams. The middle column shows the optical microscope images and normalized intensity along the output grating position. The curved surface scatters the incident beam into three separate lobes, whereas the cloaked curved surface maintains the original profile, similar to reflection from a flat surface. The experimental intensity profile agrees well with the intensity profile ( $|E_z|^2$ ) obtained from 2D simulations, which is plotted next to the spatial field magnitude ( $|E_z|$ ) in the right column.

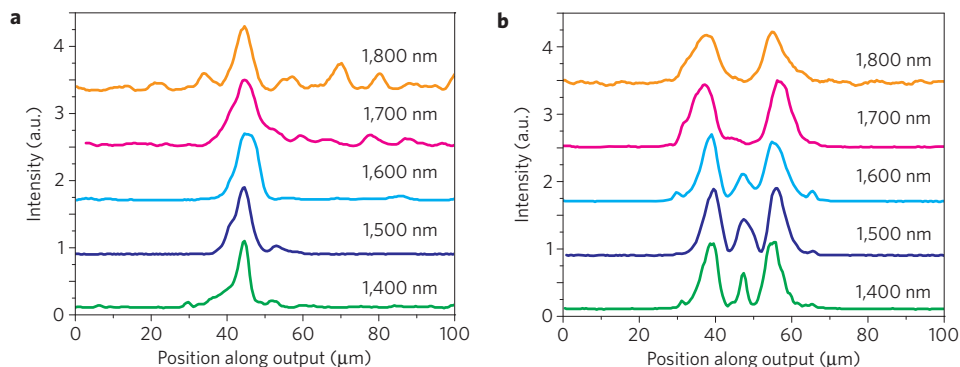


**Figure 4 | Wavelength dependence of the carpet cloak. a, b.** Plot of the intensity along the output grating for a curved reflecting surface with a cloak (**a**) and without a cloak (**b**). The cloak demonstrates broadband performance at 1,400–1,800 nm wavelengths. Distinct splitting of the incident beam is observed from the uncloaked curved surface owing to the strong scattering of the original beam.

with reactive ion etching to completely eliminate the loss associated with gallium as well as provide for much larger cloaking devices. In this case, almost perfect transmission should be attainable owing to low intrinsic loss of silicon or other dielectrics.

To obtain the bandwidth of the carpet cloak, measurements were carried out over a wide range of wavelengths. The output intensity profiles for these measurements are plotted in Fig. 4a. For a broad wavelength range from 1,400 to 1,800 nm, the beam profile shows a single peak at the output grating; that is, the cloak performance is largely unaffected by the wavelength change. At wavelengths below 1,400 nm, the cloak performance suffers owing to the fact that the wavelength in the slab waveguide ( $\lambda_0/n_{\text{Si}}$ ) becomes comparable to the hole diameter of the cloak pattern, causing increased scattering and breakdown of the effective medium approximation. The effectiveness of the optical cloak can be improved at wavelengths below 1,400 nm by using a smaller hole diameter and separation, reducing the scattering and extending the effective medium approximation to a shorter wavelength. Unlike the cloak, the bump alone exhibits a multi-peak output beam (Fig. 4b) that is clearly observed for all wavelengths, indicating the strong perturbation of the beam. The upper wavelength limit for the cloak is ultimately restricted by waveguide cutoff. However, measurements above 1,800 nm were not possible owing to the CCD sensitivity cutoff.

The experimental demonstration of cloaking at optical frequencies suggests invisibility devices are indeed in reach. The all-dielectric design reported here is isotropic and non-resonance based, therefore promising a new class of broadband and low-loss optical cloaks. This method can also be extended into an air background by incorporating non-resonant metallic elements to achieve indices smaller than one. The quasi-conformal mapping design and fabrication method presented here may also open new realms of transformation optics beyond cloaking.

*Note added in proof.* During the production stage of this letter, an unpublished report of a similar approach for optical cloaking was placed on a preprint server<sup>30</sup>.

Received 7 April 2009; accepted 20 April 2009;  
published online 29 April 2009

## References

1. Ward, A. J. & Pendry, J. B. Refraction and geometry in Maxwell's equations. *J. Mod. Opt.* **43**, 773–793 (1996).
2. Pendry, J. B., Schurig, D. & Smith, D. R. Controlling electromagnetic fields. *Science* **312**, 1780–1782 (2006).
3. Leonhardt, U. Optical conformal mapping. *Science* **312**, 1777–1780 (2006).
4. Leonhardt, U. Notes on conformal invisibility devices. *New J. Phys.* **8**, 118 (2006).

5. Smith, D. R., Padilla, W. J., Vier, D. C., Nemat-Nasser, S. C. & Schultz, S. Composite medium with simultaneously negative permeability and permittivity. *Phys. Rev. Lett.* **84**, 4184–4187 (2000).
6. Smith, D. R., Pendry, J. B. & Wiltshire, M. C. K. Metamaterials and negative refractive index. *Science* **305**, 788–792 (2004).
7. Schurig, D. *et al.* Metamaterial electromagnetic cloak at microwave frequencies. *Science* **314**, 977–980 (2006).
8. Dolin, L. S. On a possibility of comparing three-dimensional electromagnetic systems with inhomogeneous filling. *Izv. Vyssh. Uchebn. Zaved. Radiofiz.* **4**, 964–967 (1961).
9. Post, E. G. *Formal Structure of Electromagnetics; General Covariance and Electromagnetics* (Interscience, 1962).
10. O'Brien, S. & Pendry, J. B. Magnetic activity at infrared frequencies in structured metallic photonic crystals. *J. Phys. Condens. Matter* **14**, 6383–6394 (2002).
11. Zhou, J. *et al.* Saturation of the magnetic response of split-ring resonators at optical frequencies. *Phys. Rev. Lett.* **95**, 223902 (2005).
12. Ishikawa, A., Tanaka, T. & Kawata, S. Negative magnetic permeability in the visible light region. *Phys. Rev. Lett.* **95**, 237401 (2005).
13. Cai, W., Chettiar, U. K., Kildishev, A. V. & Shalaev, V. M. Optical cloaking with metamaterials. *Nature Photon.* **1**, 224–227 (2007).
14. Alu, A. & Engheta, N. Multifrequency optical invisibility cloak with layered plasmonic shells. *Phys. Rev. Lett.* **100**, 113901 (2008).
15. Li, J. & Pendry, J. B. Hiding under the carpet: A new strategy for cloaking. *Phys. Rev. Lett.* **101**, 203901 (2008).
16. Jiang, W. X. *et al.* Invisibility cloak without singularity. *Appl. Phys. Lett.* **93**, 194102 (2008).
17. Leonhardt, U. & Tyc, T. Broadband invisibility by non-euclidean cloaking. *Science* **323**, 110–112 (2009).
18. Tyc, T. & Leonhardt, U. Transmutation of singularities in optical instruments. *New J. Phys.* **10**, 115038 (2008).
19. Liu, R. *et al.* Broadband ground-plane cloak. *Science* **323**, 366–369 (2009).
20. Linden, S. *et al.* Magnetic response of metamaterials at 100 Terahertz. *Science* **306**, 1351–1353 (2004).
21. Liu, N. *et al.* Three-dimensional photonic metamaterials at optical frequencies. *Nature Mater.* **7**, 31–37 (2008).
22. Valentine, J. *et al.* Three-dimensional optical metamaterial with a negative refractive index. *Nature* **455**, 376–379 (2008).
23. Li, J., Zhang, X. & Pendry, J. *Plasmonics and Metamaterials*, OSA Technical Digest (Optical Society of America, 2008) paper MMB1.
24. Greenleaf, A., Kurylev, Y., Lassas, M. & Uhlmann, G. Electromagnetic wormholes and virtual magnetic monopoles from metamaterials. *Phys. Rev. Lett.* **99**, 183901 (2007).
25. Rahm, M., Cummer, S. A., Schurig, D., Pendry, J. B. & Smith, D. R. Optical design of reflectionless complex media by finite embedded coordinate transformations. *Phys. Rev. Lett.* **100**, 063903 (2008).
26. Kildishev, A. V. & Shalaev, V. M. Engineering space for light via transformation optics. *Opt. Lett.* **33**, 43–45 (2008).
27. Levy, U. *et al.* Inhomogeneous dielectric metamaterials with space-variant polarizability. *Phys. Rev. Lett.* **98**, 243901 (2007).
28. Liu, Z., Lee, H., Xiong, Y., Sun, C. & Zhang, X. Far-field optical hyperlens magnifying sub-diffraction-limited objects. *Science* **315**, 1686 (2007).
29. Smolyaninov, I. I., Hung, Y.-J. & Davis, C. C. Magnifying superlens in the visible frequency range. *Science* **315**, 1699–1701 (2007).
30. Gabrielli, L. H., Cardenas, J., Poitras, C. B. & Lipson, M. Cloaking at optical frequencies. Preprint at <<http://arxiv.org/abs/0904.3508>> (2009).

### Acknowledgements

We acknowledge financial support from the US Department of Energy under Contract No. DE-AC02-05CH11231 and from the US Army Research Office (ARO) MURI program 50432-PH-MUR. T.Z. acknowledges a fellowship from the Alexander von Humboldt Foundation.

### Additional information

Supplementary information accompanies this paper on [www.nature.com/naturematerials](http://www.nature.com/naturematerials). Reprints and permissions information is available online at <http://npg.nature.com/reprintsandpermissions>. Correspondence and requests for materials should be addressed to X.Z.